Skeletal Radiol (2015) 44:811–821
DOI 10.1007/s00256-015-2103-y

SCIENTIFIC ARTICLE

Radiological findings in an ancient Iranian salt mummy (Chehrābād ca. 410-350 BC)

Lena M. Öhrström · Roger Seiler · Thomas Böni · Abolfazl Aali · Thomas Stöllner · Frank J. Rühli

Received: 15 October 2014 / Revised: 26 November 2014 / Accepted: 9 January 2015 / Published online: 7 February 2015

Abstract
Objective To study pathologies, peri- and postmortal alterations as well as the general preservation state of an ancient Iranian salt mummy.
Materials and methods Several mummified remains from two different time periods (1500–2500 BP) were found in the Chehrābād salt mine in Iran. Computed tomography was performed on Salt Man #4 (410-350 BC), the best preserved out of the six salt mummies (Siemens, Sensation 16; 512×512 matrix; 0.75–5 mm slice thickness, 240-mA tube current, 120-kV tube voltage, and 0.976-mm pixel size).
Results Radiological analyses showed an excellent state of preservation of an adolescent body. Several normal variants such as aplasia of the frontal sinus as well as a rare congenital deformation of the 5th vertebral body (butterfly vertebra) have been observed. The individual shows multiple fractures, which is consistent with the theory that he died due to a collapse in the ancient salt mine.
Conclusions The salt preserved the soft tissue as well as parts of the inner organs remarkably well. However, further investigations including histology are needed to reveal additional details of the health status of this unique salt mummy.

Keywords Salt mummy · Ancient salt mine · Paleoradiology · CT · Postmortal alterations

L. M. Öhrström · R. Seiler · T. Böni · F. J. Rühli (✉)
Swiss Mummy Project, Institute of Evolutionary Medicine, University of Zurich, Winterthurerstrasse 190, 8057 Zurich, Switzerland
e-mail: frank.ruehli@iem.uzh.ch

T. Böni
Orthopedic University Hospital Balgrist, Forschstrasse 340, 8008 Zurich, Switzerland

A. Aali
Archaeological Museum of Zanjān, Emaarate Zolfaghari, Taleghani Street, Zanjān, Iran

T. Stöllner
Institut für Archäologische Wissenschaften, Ruhr Universität Bochum, Am Bergbaumuseum 31, 44791 Bochum, Germany

Present Address:
L. M. Öhrström
Institute of Diagnostic Radiology, University Hospital Zurich, Raemistrasse 100, Zurich, Switzerland

Introduction

In 1994, miners at the salt mine of Douzklah, Chehrābād, northwestern Iran, discovered remains of an ancient mummified human body (Salt Man #1, SM1) dated to the early Sassanid time period (224-651 AD) [1]. Despite this find, mining activities continued, and, in 2004, remains of a second mummified body (SM2) were discovered. In the following rescue excavations conducted by the Zanjān Cultural Heritage centre (Miras Farhangi Zanjān) during the winters of 2003/4 and 2004/5, remains of several ancient partially mummified human bodies (SM3, SM4 and SM5) as well as numerous tools and textiles were excavated [2–4]. Archeological investigations by the Miras Farhangi Zanjān revealed that the salt mine of Chehrābād was already in use in antiquity. Some human remains are carbon dated to the Achaemid (ca. 500 BC) and others to the Sassanid time period (ca. 400 AD) and the individuals most likely died during mining catastrophes in the ancient salt mine [2, 5]. Since then, the mining activities have ceased, a multidisciplinary research project with international project partners (Iranian Cultural Heritage, Handicrafts and Tourism Organisation [Zanjān Archaeological Museum/ICHHTO Zanjān], Iran, Ruhr- University of Bochum and Deutsches Bergbau Museum Bochum, University

of Oxford, University of Zurich and other partners) [6] was established, and in 2010/11 the first research field seasons were conducted. Since then, the ancient mine has been further explored, and remains of an additional salt man (SM6) have been found. A preliminary report of the ancient salt mine and the finds can be found in Aali, 2012 [2].

Archeological context

Chehrābād mine is one of few known examples of an ancient rock salt exploitation. The rock salt layers exposed to the surface by a salt dome, were exploited during two main eras, the Achaemenid period (6th–5th century BC), and later during the Sassanid period (3rd–7th century AD). During the last campaign in 2011, evidence of a third historical mining phase was discovered via a series of radiocarbon dates to the 18th to the late 19th century AD. As the salt mining debris was piled up and dumped during such a long time within the old mining galleries, it is crucial to delicately differentiate the archeological context and stratigraphy. The older two mining phases used room-and-pillar excavation, while the historical mining reworked the old galleries more irregularly. The mining technique resulted in large underground halls that became unstable. The 2004/5 and 2010/11 archeological excavations found evidence of two mining catastrophes. Some parts of the mining halls had collapsed and killed at least three Achaemenid miners between 420 and 390 BC. Further collapses occurred during the Sassanid period between the 5th and 6th century AD [2, 3, 6].

The rock salt mining debris, a mixture of rock salt, clay, gypsum, and organic remains, provided the best preservation conditions. All the samples were recorded in their stratigraphical context. Relative dating via associated archeological artifacts and AMS radiocarbon dating were consistent [2]. The whole stratigraphic sequence is an extraordinary archive for paleo-ecological and economic studies and provides a wealth of information about landscape, subsistence pattern of the mining enterprise, and the logistic concerns in running a salt mine during the Achaemenid and the Sassanid periods.

Salt mummies

Ancient human remains and their belongings are valuable sources for the study of former living conditions, mortuary practices, and the evolution of disease patterns [7]. In paleopathological and anthropological research, mummies are of particular interest, as they are often very well preserved [7–9]. Mummies are defined as human or animal remains, preserved from decay by special taphonomic conditions [7, 8]. In contrast to skeletal remains, soft tissue is widely preserved and allows for the investigation of a wide spectrum of disease, including e.g., arteriosclerosis [10], tuberculosis [11], and Chagas disease [12].

Examples of artificial mummification are known from multiple cultures and time periods all over the world. Alternatively, naturally mummified historic human remains are very rare and thus can act as unique examples of certain cultures and time periods. They can be found in different environmental conditions such as in deserts, ice, or areas with permafrost, bogs, caves, salt, or crypts [13]. The extremely arid and hot/cold conditions in deserts lead to a rapid dehydration of the body, thus stopping the decomposition process. Cold conditions in ice or areas with permafrost can slow down the chemical processes or lead to freeze-drying. In peat bogs, the chemical composition and the almost completely anaerobic conditions can prevent putrefaction [14]. Salt-rich environments are found in salt deserts, salt lakes, seashores, or salt mines. The hygroscopic properties of the salt can lead to mummification by dehydration. Bacterial growth is inhibited and protects the tissue from decomposition [15].

Previously, the only known examples of salt mummies were those of the salt mines in Hallstatt, Austria [7, 13, 16] and Hallein-Dürrnberg [17]. Several mummified bodies were found in the 16th to 18th centuries AD. Unfortunately these finds are no longer available, since they were immediately reburied after discovery [16, 17].

The Iranian Salt Men are presently the only available salt mummies worldwide. The salt content of the soil preserved their remains in a unique form. To study theses precious specimens, non-invasive analyses such as diagnostic imaging methods are desirable. Currently established diagnostic imaging technologies to study ancient remains include X-ray and computed tomography (CT) [18]. The radiological examination of the Salt Man #4 forms part of the *Interdisciplinary Chehrābād Douzlakh Project,* a multidisciplinary study of the Douzlakh salt mine and its salt men, including archeobotany, archeozoology, ancient DNA analysis, geomorphology, isotopic analysis, mining archaeology, physical anthropology, and textile analysis.

Within the framework of the *Interdisciplinary Chehrābād Douzlakh Project*, CT imaging was performed on the Iranian Salt Man #4, the best-preserved salt mummy of the six in order to study pathologies, peri- and postmortal alterations as well as the general preservation state within the salt. Here, we report the radiological findings in Salt Man #4.

Materials and methods

Site The salt mine of Douzlakh, Chehrābād is located in northwestern Iran, in the Zanjān province, 75 km from the city of Zanjān, 1 km south of Hamzehli village, 1,350 m above sea level, N 36°54′52″, E 47°51′25″ (Fig. 1). Salt Man #4 was discovered in Trench A at a depth of 4 m in winter 2004 during the first rescue excavation. The excavation was conducted by the Zanjān Cultural Heritage centre (Miras Farhangi

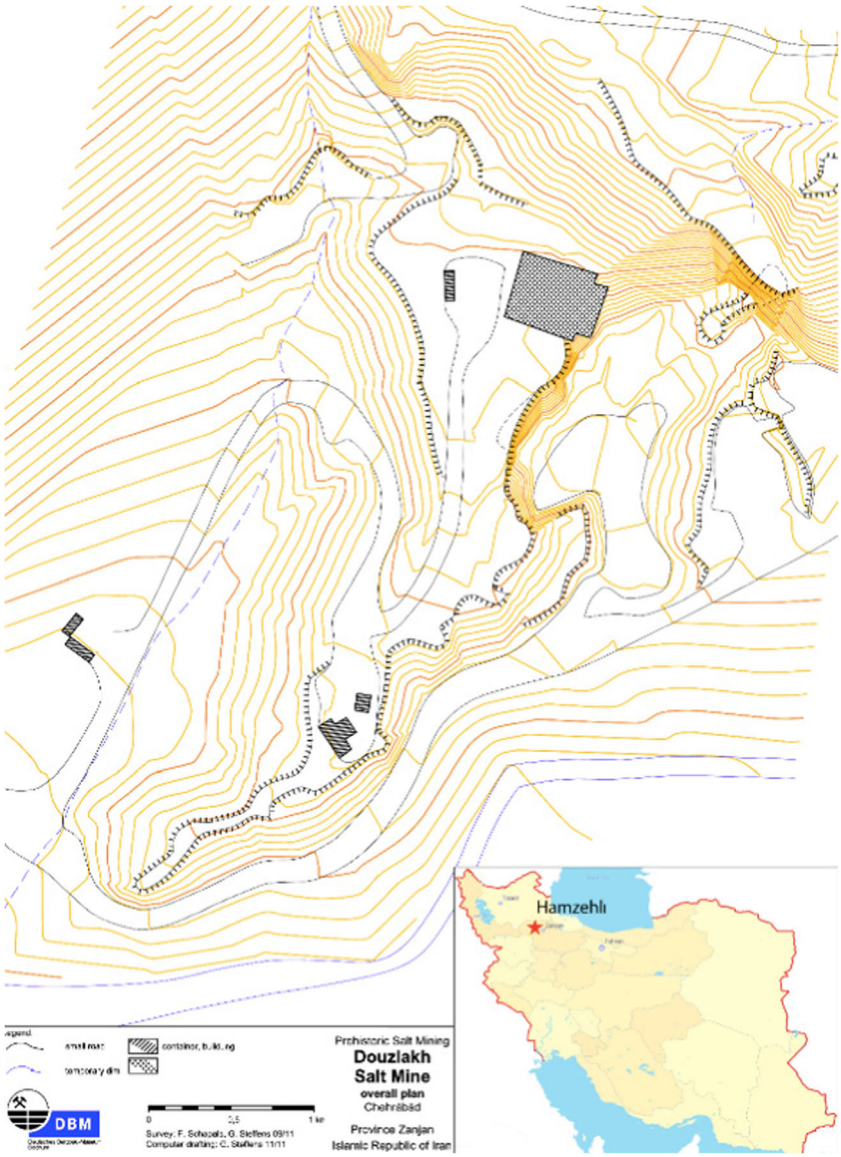

Fig. 1 Site map of the ancient Chehrābād salt mine and its location within Iran (graphics: Deutsches Bergbau-Museum, Bochum, Germany)

Zanjān / http://www.saltmen-iran.com/tiki-index.php) and supervised by Abolfazl Aali, the director of the archaeological museum in Zanjān.

Material Salt Man #4 is a 170–175 cm tall male. He has no beard, and his hair is brown and cut short. The mummy is fully clothed (woolen trousers, a long knee-length robe and leather shoes) and wears a metal earring on the right ear. A textile rope is fixed to the belt around the waist and a red-brown colored pelt coat is attached to the right shoulder (Fig. 2). The body was found in a prone position, facedown, both arms were bent, the right leg extended and the left leg flexed. Besides the mummy, several objects were found including two small pitchers, several textile ropes and leather pieces, and a metal knife in a leather sheath attached to the belt [2]. The salt mummy #4 is radiocarbon dated to 405–380 cal BC [5], which corresponds to the end of the Achaemenid time period. The clothing has been assigned to Median in style [19]. According to Ramaroli [19], Salt Man #4 appears isotopically different than the other remains of the salt mine and probably originated in the Persian Gulf or the Caspian or Black Sea.

The mummified specimen is currently on exhibit in the Archaeological Museum of Zanjān, Zanjān, Iran.

Methods The Iranian Salt Man #4 was examined by using a clinical CT scanner (Siemens, Sensation 16) at the Pardis Noor Medical Imaging Center, Tehran, Iran in September 2011. Imaging parameters were as follows: 512×512 matrix; 0.75–5-mm slice thickness, 240-mA tube current, 120-kV tube voltage, and 0.976-mm pixel spacing.

No full-body scan is available since the mummy did not entirely fit into the CT scanner. In total, 47 series (with different slice thickness and images/series) were obtained including continuous scans of head, chest, and abdomen until the level

Fig. 2 **a** Salt Man#4 as found in the salt mine. **b** Frontal view of Salt Man#4 (pictures: Archaeological Museum of Zanjan, Iran and Deutsches Bergbaumuseum Bochum, Germany)

Fig. 3 Bone status of the right partially fractured and malpositioned hand. *Arrows* indicate the open epiphyses of the radial bone (*R*), the metacarpal bone 1 (*MC I*) and of the proximal phalanx. *Arrowhead* distal undisplaced radius fracture

of thoracic vertebra 12 with both upper extremities (missing elbows on both sides). The pelvis (consisting of 6–10 images per scan only) as well as the right leg were scanned separately. Parts of the left foot are visible on the hip scans.

The datasets were processed with OsiriX–64 bit (version 5.8.5) software, including multi-planar reconstructions (MPR) and three-dimensional volume rendering (3D VR). Age determination included dental status and the bone status of the hand, according to Greulich and Pyle [20], as well as the bone status of the right foot, according to Hoerr et al. [21].

Radiological findings

General findings The individual is not full-grown: epiphyseal plates remain open in various bones, including the humerus, femur, tibia, fibula, ulna, and radius (Figs. 3, 4a and 9c). While the epiphyses of all proximal phalanges remain open, the epiphyses of the metacarpal bones I–V are about to begin fusion. According to Greulich and Pyle [20], the bone status of the right hand indicates an age of 15–15.5 years (Fig. 3). According to Hoerr et al. [21], the bone status of the right foot corresponds to plate 27/28 and indicates a skeleton age of 15–16 years (Fig. 4a). The dental state indicates an estimated age-at-death between 15 and 17 years (see below). The mummy shows traces of massive external pressure and thus multiple perimortem fractures. Radiointense structures (ca. 1,400 HU) are visible at multiple locations around the body (differential diagnosis: soil; Figs. 5 and 11). The mummy wears clothes and shoes, which are remarkably well preserved (Figs. 2 and 4b). Two small pitchers and a knife sheath are found beside the hip (Figs. 2 and 11).

Skull The skull has multiple fractures and is partially compressed. The occipital as well as both parietals show multiple comminuted displaced fractures. The right maxillary sinus is laterally fractured. The right orbit is laterally and inferiorly fractured ("blow-out fracture"). The clivus is shifted caudally, the sella turcica is unidentifiable, and the sphenoidal sinus is slightly damaged, showing multiple small fracture lines (Figs. 5, 6a and b). In the cranial cavity, remains of the brain (60–260 HU) are visible frontally, and remnants of the dura, especially the falx cerebri, are observable too (Figs. 5 and 6b). The frontal sinuses are not pneumatized, whereas maxillary sinuses, sphenoidal sinus, and mastoidal processes are well pneumatized. In the orbit, remnants of the eyeball as well as of the eye muscles and intact optical nerves are recognizable (Fig. 5c). The mummy wears an earring on the right ear (ca. 3,070 HU), which leads to surrounding technical artefacts (Fig. 6a). A deviation of the nasal septum to the left is visible and the mandible is fractured on the right side.

Dentition The mummy's dentition is complete except for the non-developed third molars. The second molar's root growth is incomplete, giving an estimated age of ca. 15–17 years. The

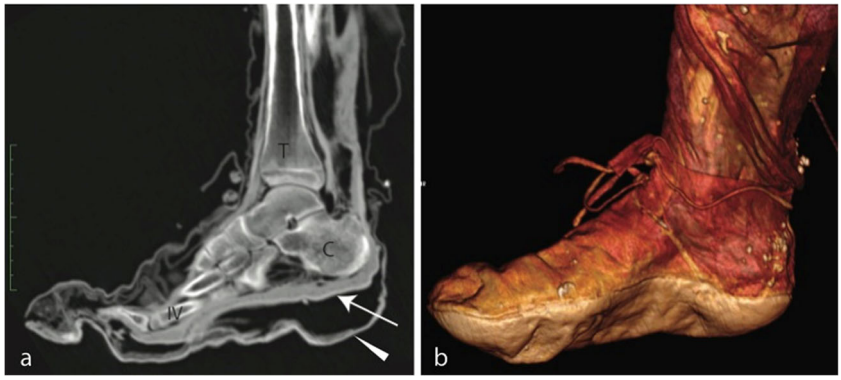

Fig. 4 **a** Sagittal slice and **b** 3D reconstruction of the right foot. Note the very well preserved leather shoe (*arrowhead*) and the open ephyiphyses in the tibial bone (*T*). *C* calcaneus; *IV* metatarsal bone 4; *arrow* skin

right second deciduous maxillary molar persists with highly resorbed roots. Hence, the second premolar erupts toward the palate. The first left mandibular molar shows small occlusal caries in the dentine underneath the central fissure (Fig. 7). Abrasion is generally very mild or absent. A postmortem fracture of the mandibula on the right side as well as multiple postmortem fractures of the crowns of the lower front teeth and the first premolars are visible. Avulsion and consecutive retro-dislocation of mid-face area lead to mandibular prognathism.

Spine The vertebral column is malpositioned. The cervical part is axially compressed, which probably led to the present cervical hyperlordosis (Figs. 5a). The atlanto-occipital joint, however, is intact. The thoracic spine shows a postural scoliosis. The thoracic vertebra no 5 shows a midsagittal bony crest in the posterior face of the vertebral body throughout the vertebra and a depression of the superior and inferior end plate leading to a mild form of a *butterfly vertebra,* which is caused by a congenital malformation (Fig. 8). Several intervertebral discs show a vacuum phenomenon (Figs. 9b and c). The rest of the vertebral column is intact and shows a normal alignment. Remnants of spinal nerves are found in the spinal canal and the dura is partially detached from the vertebrae, which is particularly visible in the lumbar region (Fig. 9).

Chest The chest is severely compressed (Fig. 10a), which leads to a narrowed anteroposterior diameter of the thorax as well as to dislocated clavicles and shoulders on both sides. The ribs are multiply fractured on both sides (level 4–10 on both sides as well as the 2nd rib on the left side), including segmental fractures (Fig. 6c), and several costo-vertebral joints are luxated on the left side (level 3–8). The clavicle is fractured on both sides (left: at c. proximal third; right: in the middle), and both scapulae bear multiple fractures. The dehydrated lungs are collapsed to a great extent and small tissue bands are observable throughout the thorax. A presumable heart residue is identifiable in the former mediastinum. In the right thoracic cavity at the level of the thoracic vertebra 9, a homogenous structure of undefinable tissue is visible (differential diagnosis: lung, exudate; range, −236 to +379 HU). Parts of the damaged diaphragm are visible at certain locations (Fig. 9).

Abdominopelvic cavity In the abdomen, some remnants of the intestine and possible liver remains are visible (maximal

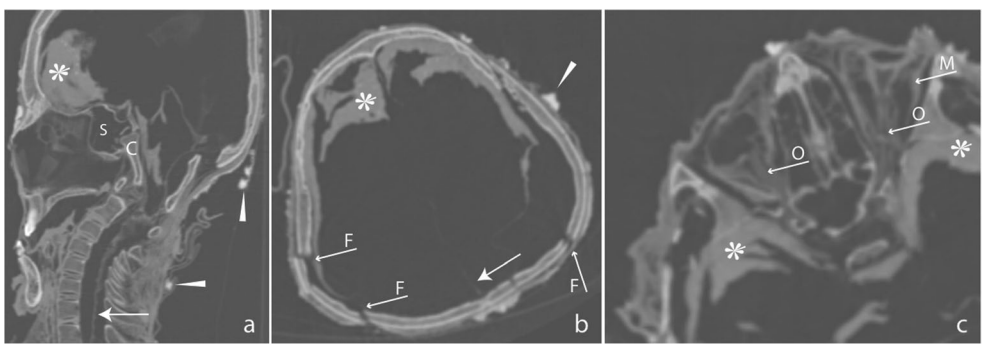

Fig. 5 Head and cervical column, **a** sagittal slice, **b** axial slice. Note the translocated clivus (*C*), the multiple fractures (*F*) and the slightly damaged sphenoidal sinus (*S*) as well as the brain remnants (*). **c** Axial slice of the well-preserved orbit region with intact optical nerve (*O*) and remnants of the orbital muscles (*M*). Note also the dura remnants and remains of the falx cerebri (*arrow*); *arrowhead* radiointense structure, most likely differential diagnosis: soil

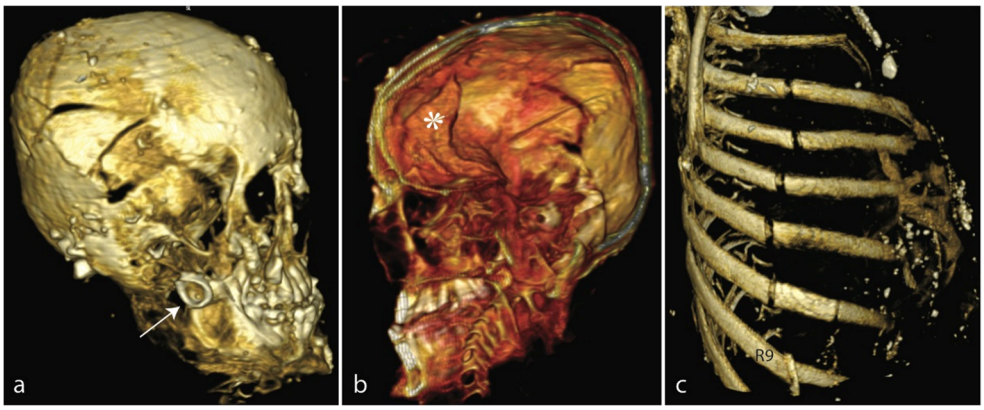

Fig. 6 3D reconstructions of **a** head with multiple fractures on temporal and parietal bone, **b** interior view of the cranial cavity with frontally located brain remnants (*star*), and **c** chest with multiple rib fractures on the right side. *Arrow* earring; *R9* 9th rib

dimensions: 7 (right-left);×4.8 (cranio-caudal)×3 (ap) cm; range: −613 to +185 HU). In the upper left abdomen, additional liver remains are observable (differential diagnosis: spleen remains; max. dimensions: 1.5 (right-left)×2.5 (cranio-caudal)×1.5 (ap) cm; Figs. 9c, d and 10b). In the pelvis, presumed remnants of the colon and the rectum are seen (Fig. 11). No other organs such as kidneys or pancreas are recognizable and no inner or outer sexual organs can be identified. Skin and muscle tissue are identifiable.

Hip The left hip is subluxated, the acetabulum shows multiple fractures on both sides and the pubic symphysis is disrupted. The left ischium bone is fractured, the left iliosacral joint is luxated, and the joint space of the right iliosacral joint is broadened. A possible detachment of the labrum and a small cyst (5 mm) with a sclerotic margin in the right ischium bone are observable (Fig. 11).

Upper and lower extremities The extremities show multiple fractures, including a right distal comminuted radius fracture (Fig. 3), a right comminuted and displaced metacarpal II fracture, a right metacarpal III fracture and a left comminuted proximal humerus fracture. Furthermore, a left distal intraepiphyseal femur fracture (condyles, Fig. 9c), and a right metaphyseal tibia fracture are visible. The right ankle is well positioned (Fig. 4), however the right digits I–V are malpositioned (hyperextension in metatarso-phalangeal joints). The left ankle cannot be assessed, as this part has not been imaged. The right wrist is deviated in ulnar direction and the digits are in a flexed position. The left hand is malpostitioned; while the left wrist is fully extended, the metacarpophalangeal and interdigital joints are partly flexed and hyperextended.

Discussion

State of preservation Salt Man #4 shows a remarkable state of preservation. In contrast to the other Chehrābād salt men, the body is intact and completely mummified [2]. The soft tissue is largely preserved allowing for the identification of numerous tissues. The muscles are especially well preserved. Compared to other mummification types, such as Egyptian and Peruvian mummies or bog bodies, as seen in Sydler et al. [22], the level of shrinkage is rather low and the muscles are

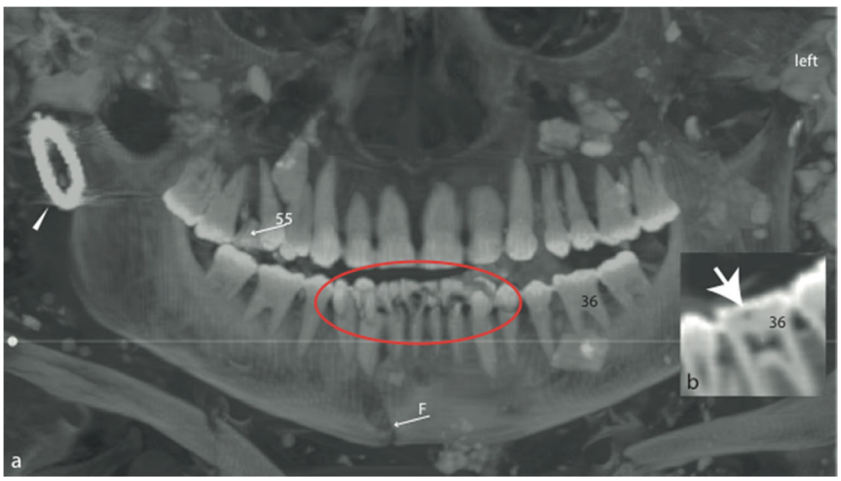

Fig. 7 **a** 3D curved multi-planar reconstruction of the dentition. Note the persistence of the right second deciduous maxillar molar (*55*). *F* fractured mandibula, *arrowhead* earring. Note also the multiple postmortem fractures of dental crowns (*surrounded*). **b** Occlusional caries (*arrow*) of first left mandibular molar (*36*)

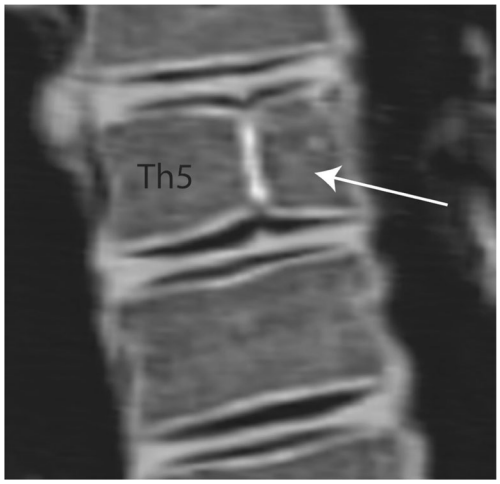

Fig. 8 Coronal slice of part of the thoracal vertebral column. Note the midsagittal bony crest as well as the depression of the superior and inferior endplate of thoracic vertebra 5

relatively undistorted. Various personal belongings, which have been found along with the mummy, are all very well preserved.

The taphonomic conditions, including the hygroscopic properties of the salt as well as the arid environment led to dehydration of the tissue, which inhibited the bacterial growth and stopped putrefaction [15]. It is crucial that dehydration starts before decomposition begins. This explains why most natural mummies are found in arid environments [7, 23, 24]. Similar conditions were probably the case in artificial mummification techniques in ancient Egypt.

The CT scans revealed multiple peri- and postmortem alterations of the body, including evidence of massive external pressure. These alterations suggest a severe blunt-force trauma causing high-energy fractures, which is most likely caused by a collapse of the ancient salt mine. Similar traumatic causes of death with severe mechanical injuries are described in case reports from mining victims, e.g., coal miners from Poland [25]. Traumatic injury patterns including multiple fractured skeletons are also described in skeletal remains of a 19th century landslide victims [26].

Organ preservation The identification of the internal organs remains difficult. They generally show little anatomic similarity to normal organs. Due to the desiccation process, they are shrunken and deformed, a common phenomenon in both natural and artificial mummies [7, 27]. Furthermore, the thoracic and abdominal organs might be dislocated, since the chest and abdomen are strongly compressed. However, several organ remains are identifiable, including brain, lung, presumed heart, liver, gut, and rectum.

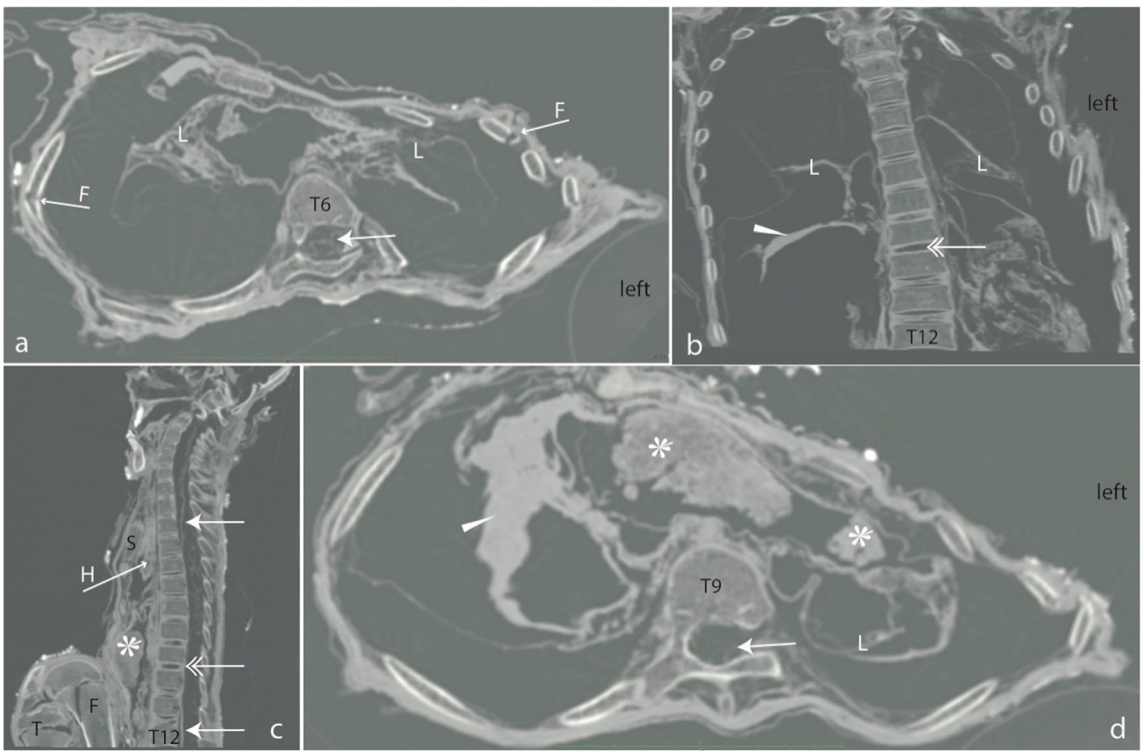

Fig. 9 **a** Axial slice at the level of thoracic vertebra 6 and **b** coronal slice of the thoracic cavity showing remnants of the lung (*L*). **c** Sagittal slice and **d** axial slice at the level of the ninth thoracic vertebra showing remnants of the lung (*L*), heart (*H*), and of the liver (*star*). Note also remnants of the dura (*arrow*), the vacuum Phenomenon in some intervertebral discs (*double arrow*) and the fractured distal left femur (*F*). Separation of the epiphyseal plate in the proximal left tibia (*T*) suggests, that the epiphyseal plate was not closed at death. *S* sternum; *F arrow* fractured ribs; *arrowhead* unclear structure, likely differential diagnoses: lung tissue or exudate

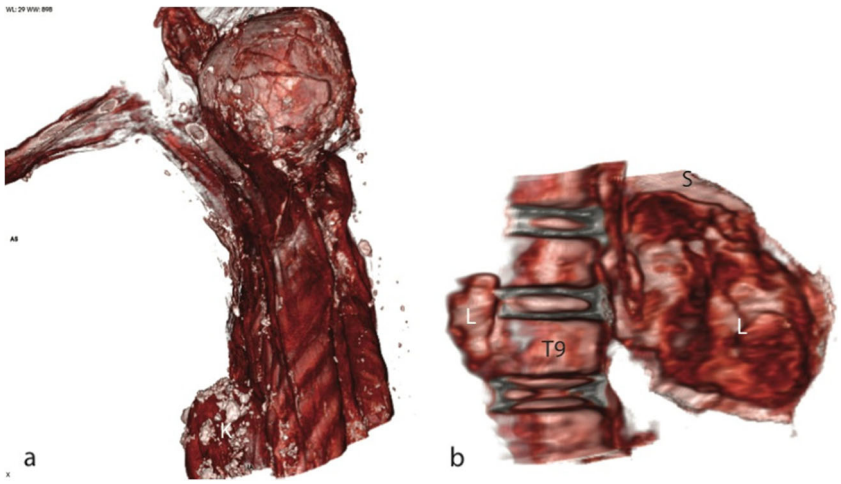

Fig. 10 3D reconstruction of the **a** massively compressed trunk and the multiply fractured skull and **b** part of the spine and presumed liver remnants (*L*), located in frontal right abdominal cavity. View from diagonal right. *K* knee, *S* skin

The brain is extremely shrunken and the different brain parts are indistinguishable. Similarly, in Peruvian and Egyptian mummies without brain removal, the cranial cavity has a comparable appearance: dura remnants are often recognizable, while the brain itself is only minimally preserved [28].

The smaller structure of similar density in the left abdomen most likely forms part of the ruptured liver. Since the liver has a soft consistency, it easily ruptures in accidents with blunt-force abdominal trauma [29], which was probably this case. Similar cases have been described in coal mine victims [30]. Nevertheless, it might also be spleen tissue, although this is rather unlikely since the spleen is an enzyme-rich organ [31] that usually autolyses rapidly after death. In contrast to the spleen, liver tissue is commonly preserved in ancient mummies, such as in the Iceman [27] and in South America [7] and in Korea [13, 32].

The pancreas is rarely found in mummies, since it undergoes rapid self-digestion. Renal structures usually autolyses shortly after death [7, 15] too. In conclusion, the radiologic and macroscopic identification of internal organs in mummies is difficult in both, historic as well as forensic cases [23]. Exemplary, histological analyses could further clarify tissue identification. [33]. These investigations, however, are invasive, which is usually undesirable in historic mummies.

Age-at-death Age determination from CT scans of skeletal remains is difficult, particularly in adults [34]. In juvenile bodies, however, age determination is more accurate [35]. The determination of the skeletal age of juvenile bodies on a plain hand X-ray according to Greulich and Pyle [20] is widely accepted. Several studies showed that bone maturity in this age group generally corresponds with the age [36, 37]. The

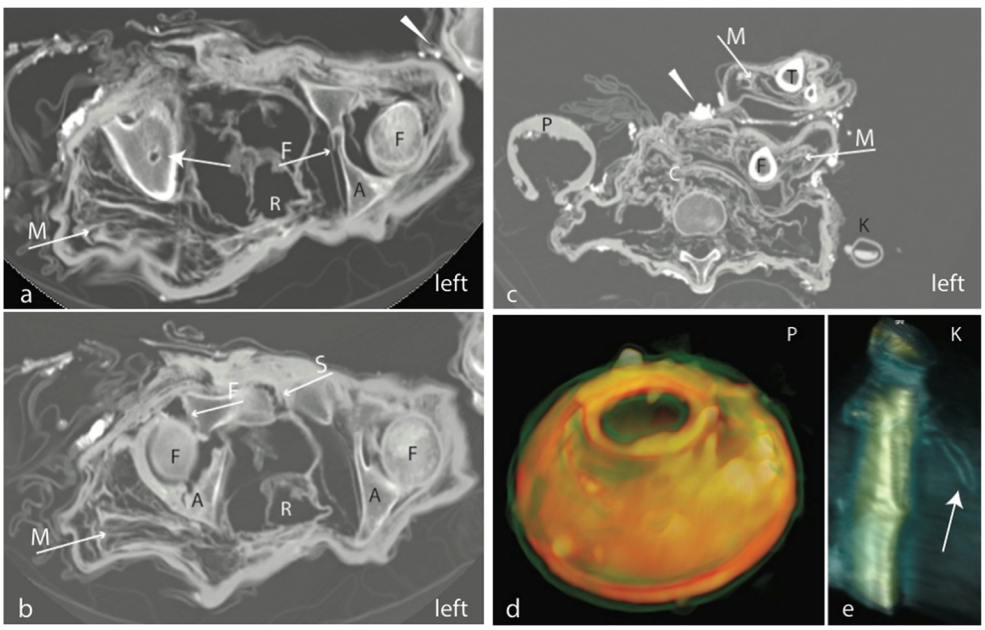

Fig. 11 **a**, **b** Axial slices of the hip region showing the multiple fractured acetabulum (*F arrow*) on both sides, a pubic symphysis disruption (*S arrow*) and a cyst in the right ischium (*arrow*). **c** Axial slice at lower lumbar region; note the conserved muscles (*M arrow*) of the lower left extremity. Presumed remnants of the colon (*C*) cannot be further differentiated. *P* pitcher; *F* femoral head; *A* acetabulum, *R* presumed remnants of rectum; *arrowhead* radiointense structure, differential diagnosis: soil. **d**, **e** 3D reconstructions of the pitcher and of a metal knife in a leather sleeve. *Arrow* indicates a band fixed to the belt

Study Group on Forensic Age Diagnostics suggests for age estimations in living individuals' left hand X-rays, physical examination, and dental status as well as dental X-ray [38]. If the skeletal development of the hand is already completed, the clavicle should be analyzed radiologically as well [39]. Age determination in the Iranian salt mummy is complicated because the skeleton is partly deformed and destroyed. Since both hands of the Iranian body are fractured and malpositioned, the right foot was included for skeletal age determination. Combined with the dental findings, an age of 15–16 years seems reasonable. It has to be taken into account that age determination in historic remains and of people of different ethnic origin might differ, however the used multiple method approach is a current standard for such enigmatic cases.

Dentition and food The salt mummy shows few caries and little abrasion, which is mainly explained by the adolescent age. However, the caries already present at this young age could cause problems in the long term. Heavy abrasion, however, could stop caries formation at the occlusal surface [40], which is a likely occurrence in desert populations. Nevertheless, a larger sample size of adult individuals would be needed to answer this question. The food consumed by Salt Man #4 was probably abrasive, however no final conclusion can be drawn from one single young individual.

Normal variants and pathologies Salt Man #4 shows a bilateral absence of the frontal sinus. While the frontal sinuses are the last pneumatized paranasal sinuses, they are normally fully developed after puberty [41]. Aplasia of the frontal sinus occurs bilaterally in approximately 5 % of cases [42], yet vary in different populations [43–45]. Most cases are asymptomatic and diagnosed incidentally.

The agenesis of the third molars is not unusual and up to 25 % of the population may miss at least one third molar [46].

The 5th vertebra shows a mild form of a sagittal cleft centrum a (butterfly vertebra) [47]. This defect is caused by a congenital malformation, due to failure of the notochord to regress. It is seen in the thoracic or lumbar spine and usually only affects one vertebra. This malformation is rarely seen and occurs more often in males than in females [48]. There are a few case reports of sagittal cleft centrum in prehistoric specimen as e.g., in Peru [49] or Canada [50]. It may be associated with defects in the gastrointestinal tract, central nervous system, or with other vertebral defects or even with rare syndromes such as Alagille syndrome [51] or the Pfeiffer's syndrome [52]. The Iranian salt mummy, however, shows none of these associated defects as far as determinable with the present status of preservation. Usually this congenital anomaly is asymptomatic and an incidental finding only; however it might lead to scoliosis or kyphosis and increase the risk of disc herniation [53].

In the right lower thoracic cavity, a radiodense structure is not clearly identifiable. It could be an exudate, differential diagnosis: hemorrhage, pneumonia, and might form part of an intra-alveolar hemorrhage, as described previously in coal mining accidents [54] and in an Egyptian mummy [55]. However, more detailed analyses including histology would be needed to define the structure and also to differentiate if the injury occurred intravitally or peri-mortally [56].

The small cyst found in the right ischium is most likely a solitary bone cyst [57], which probably had no clinical importance. No Harris lines, a debated indicator of general stress [58], are detected in the salt mummy.

Cause of death Salt Man #4 most likely died during a mining accident. Therefore, he probably represents a miner, or a mine visitor. The collapse of the ancient salt mine lead to an extensive blunt-force trauma, causing deformation and multiple high-energy fractures. Blunt-force trauma can compress the rib cage, contuse and rupture internal organs and vessels, and disrupt trachea or bronchi [59]. Concurrence of causes of death might also have played a role [54].

Impact of radiological investigations of mummies Non-invasive methods such as X-ray and CT are standard methods for the investigation of skeletons and mummies [18, 60]. Since these historic remains are most valuable, their integrity should be guaranteed. Radiological investigations also give insights into the preservation state of mummified remains. This reveals interesting information about the mummification in different taphonomic conditions, including natural (e.g., Iceman) and artificial mummification (e.g., ancient Egypt or the Capuchin Catacombs, Sicily) [61].

The analysis of mummified remains widely differs from analyses of clinical CT scans. Mummified tissue is difficult to identify due to multiple postmortem alterations [8, 18, 60]. For instance, the density of the tissue, as reflected by Hounsfield Units varies widely between mummies and within the same tissue type [62]. Unlike in clinical CTs, there are no reliable reference data for comparison. Soft tissue preservation varies between mummification types as described in Sydler et al. [22]. Diagnoses are difficult, since the tissue altered due to dehydration and also medical reports are lacking.

Study limitations Some limitations of the present radiological examination have to be taken into account. Due to the mummy's posture, a full body scan was not possible, so that the mummy had to be scanned in parts and some parts were not imaged at all. Some of the series include only a few images and are difficult to interpret as no continuous dataset can be analyzed (for details, see the Materials and methods section). Radiological analyses are complicated since the body shows signs of massive pressure and the tissue is shrunken and often deformed due to dehydration. In addition, there are no data of

similar mummies for comparison, which implies that the radiological analyses cannot be fully validated.

In conclusion, the radiological examination clearly shows the remarkable state of preservation of Salt Man #4, which presently is the only complete preserved example of a salt mummy worldwide. *The Chehrābād Salt Mine Project* is ongoing and will hopefully give us further insight into the living circumstances in the nowadays Iranian region more than 2,000 years ago.

Acknowledgments We especially thank Shahram Aghlaghpour (Tehrān) for performing the CT Multislice scan. We further want to thank the DFG, Germany, the Miras Farhangi Zanjān, Iran, the Mäxi foundation, Zurich, Switzerland, and the Research Laboratory of Arts and Humanities (University of Oxford) for financial support and Michael Campana, Institute of Evolutionary Medicine, University of Zurich for proofreading the manuscript.

Funding The Salt Mine Exploration Project is a collaboration including the Iranian authorities, represented by the ICAR (Iranian Centre of Archaeological Research/ICHTO), the Ruhr University of Bochum, Institute for Archaeological Studies and the Deutsches Bergbau-Museum Bochum as the main project partner as well as further partners from Zurich, Oxford, Paris, Besançon and Tehran. The current fieldwork is financed by the DFG (DFG-Grant no: STO 458/12-1). Additional activities of the different project partners are supported by Miras Farhangi Zanjān, the Mäxi-Stiftung, Zurich and the Research Laboratory of Arts and Humanities (University of Oxford).

Conflict of interest The authors declare that they have no conflicts of interest.

References

1. RCCCR. Salt man. Scientific investigations carried out on salt man mummified remains and its artifacts. Tehran Res Cent Conserv Cult Reli. 1998.
2. Aali A, Stöllner T, Abar A, Rühli F. The salt men of Iran: the salt mine of Douzlakh, Chehrabad. Archäologisches Korrespondenzblatt. 42/1:61–8.
3. Aali A. Salt men. Tehran: Iranian Center for Archaeological Research, ICHTO; 2005.
4. Hadian M, Good I, Pollard AM, Zhang X, Laursen R. Textiles from Douzlakh salt mine at Chehr Abad, Iran: a technical and contextual study of late pre-Islamic Iranian textiles. 2012;19:152–73.
5. Pollard AM, Brothwell DR, Aali A, Buckley S, Fazeli H, Hadian Dehkordi M, Holden T, Jones AKG, Shokouhi JJ, Vatandoust R, Wilson AS. Below the salt: a preliminary study of the dating and biology of five salt-preserved bodies from Zanjan province, Iran. Iran. 2008;46:135–50.
6. Aali A, Abar A, Boenke N, Pollard M, Rühli F, Stöllner T. Ancient salt mining and salt men: the interdisciplinary Chehrabad Douzlakh project in north-western Iran. In collaboration with Don Brothwell, Irene Good, Matthieu Le Bailly, Karl Link, Marjan Mashkour, Gholamreza Mowlavi, Masoud Nezamabadi, Hamed Vahdati. Antiq. Proj. Gall. http://antiquity.ac.uk/projgall/aali333/.
7. Aufderheide AC. The scientific study of mummies. Cambridge: Cambridge University Press; 2003.
8. Lynnerup N. Mummies. Am J Phys Anthropol 2007; Suppl 45:162–90.
9. Cockburn A, Cockburn E. Mummies, Disease and Ancient Cultures. Cambridge: Cambridge University Press; 1980.
10. Thompson RC, Allam AH, Lombardi GP, Wann LS, Sutherland ML, Sutherland JD, et al. Atherosclerosis across 4,000 years of human history: the Horus study of four ancient populations. Lancet. 2013;381:1211–22.
11. Zink AR, Sola C, Reischl U, Grabner W, Rastogi N, Wolf H, et al. Characterization of Mycobacterium tuberculosis complex DNAs from Egyptian mummies by spoligotyping. J Clin Microbiol. 2003;41:359–67.
12. Guhl F, Jaramillo C, Vallejo GA, Cardenas AAF, Aufderheide A. Chagas disease and human migration. Mem Inst Oswaldo Cruz. 2000;95:553–5.
13. Rosendahl W. Natürliche Mumifizierung. In: Wieczorek A, Tellenbach M RW, editors. Mumien -der Traum vom ewigen Leban. Verlag Philipp von Zabern, Mainz; 2007. p. 23–33.
14. Fisher C. Bog bodies of Denmark and northwestern Europe. In: Cockburn ACE, Reyman TA, editors. Mummies, Dis. Anc. Cult. Cambridge: Cambridge University Press; 1998. p. 237–62.
15. Powers RH. Forensic Science and Medicine. The Decomposition of Human Remains. In: Jeremy R, Dean DE, Powers RHP, editors. Forensic Med. Low. Extrem. Humana Press; 2005. p. 3–15.
16. Barth F. Salzbergwerk Hallstatt. Quellen und Literaturauszüge zum Mann im Salz. Hallstatt; 1989.
17. Schatteiner J, Stöllner T. Männer im Salz - Verunglückte Knappen. Grubenunglücke und Arbeitsunfälle im Dürrnberger Salzbergbau. Der Anschnitt. 2001;53:71–9.
18. Lynnerup N. Methods in mummy research. Anthropol Anz. 2009;67:357–84.
19. Ramaroli V, Hamilton J, Ditchfield P, Fazeli H, Aali A, Coningham RAE, et al. The Chehr Abad "Salt men" and the isotopic ecology of humans in ancient Iran. Am J Phys Anthropol. 2010;143:343–54.
20. Greulich W, Pyle S. Radiographic atlas of skeletal development of the hand and wrist. 2nd ed. Stanford: Stanford University Press; 1959.
21. Hoerr N, Pyle I, Francis C. Radiographic atlas of skeletal development of the foot and ankle: a standard of reference. Charles C Thomas: Springfield; 1962.
22. Sydler C, Öhrström L, Rosendahl W, Woitek U, Rühli F. CT-based assessment of relative soft tissue alteration in different types of ancient mummies. Anat. Rec. Spec. Issue Mummies. Press.
23. Campobasso CP, Falamingo R, Grattagliano I, Vinci F. The mummified corpse in a domestic setting. Am. J. forensic Med. Pathol. Off. Publ. Natl. Assoc. Med. Exam. 2009. p. 307–10.
24. Papageorgopoulou C, Shved N, Wanek J, Rühli FJ. Modeling ancient Egyptian mummification on fresh human tissue: macroscopic and histological aspects. Anat. Rec. Spec. Issue Mummies. Press.
25. Kobek M, Jankowski Z, Chowaniec C, Jabłoński C, Gaszczyk-Ozarowski Z. Assessment of the cause and mode of death of victims of a mass industrial accident in the Halemba coal mine. Forensic Sci Int Suppl Ser. 2009;1:83–7.
26. Meyer S, Reichlin T, Rühli F HM. Skelettfunde aus Harmettlen, Arth-Goldau, Opfer des Bergsturzes von 1806. Bull Soc Suisse Anthr. 19/1, 2013. 2013.
27. Murphy WA, Nedden DDz, Gostner P, Knapp R, Recheis W, Seidler H. The iceman: discovery and imaging. Radiology. 2003;226:614–29.
28. Wade AD, Nelson AJ, Garvin GJ. A synthetic radiological study of brain treatment in ancient Egyptian mummies. HOMO- J Comput Hum Biol. 2011;62:248–69.
29. Shao Y, Zou D, Li Z, Wan L, Qin Z, Liu N, et al. Blunt liver injury with intact ribs under impacts on the abdomen: a biomechanical investigation. PLoS One. 2013;8:e52366.
30. Chowaniec C, Kobek M, Chowaniec M, Skowronek R, Nowicka J. [The evaluation of the mechanism and cause of death of mine

rescuers during the group accident in the Niwka-Modrzejów Coal Mine in Sosnowiec in 1998]. Arch Med Sadowej Kryminol. 2011;61:319–30.
31. Aufderheide A. The scientific study of mummies. Cambridge: Cambridge University Press; 2003. p. 320.
32. Shin DH, Choi YH, Shin K-J, Han GR, Youn M, Kim C-Y, et al. Radiological analysis on a mummy from a medieval tomb in Korea. Ann Anat. 2003;185:377–82.
33. Schulz F, Tsokos M, Püsche K. Natürliche Mumifikation im häuslichen Milieu. Rechtsmedizin. 1999;10:32–8.
34. Grabherr S, Cooper C, Ulrich-Bochsler S, Uldin T, Ross S, Oesterhelweg L, et al. Estimation of sex and age of "virtual skeletons"—a feasibility study. Eur Radiol. 2009;19:419–29.
35. Franklin D. Forensic age estimation in human skeletal remains: current concepts and future directions. Leg Med (Tokyo). 2010;12:1–7.
36. Hackman L, Black S. The reliability of the Greulich and Pyle atlas when applied to a modern Scottish population. J Forensic Sci. 2013;58:114–9.
37. De Donno A, Santoro V, Lubelli S, Marrone M, Lozito P, Introna F. Age assessment using the Greulich and Pyle method on a heterogeneous sample of 300 Italian healthy and pathologic subjects. Forensic Sci Int. 2013;229.
38. Schmeling A, Grundmann C, Fuhrmann A, Kaatsch HJ, Knell B, Ramsthaler F, et al. Criteria for age estimation in living individuals. Int J Legal Med. 2008;122:457–60.
39. Kellinghaus M, Schulz R, Vieth V, Schmidt S, Schmeling A. Forensic age estimation in living subjects based on the ossification status of the medial clavicular epiphysis as revealed by thin-slice multidetector computed tomography. Int J Legal Med. 2010;142:149–54.
40. Kaidonis JA. Tooth wear: the view of the anthropologist. Clin Oral Investig 2008;12 Suppl 1:S21–S26.
41. Ma YX, Zhang WJ, Yan ZH, He JW, Cheng XJ, Wang YJ, et al. [Normal pneumatization time of paranasal sinuses in 799 children: evaluation with magnetic resonance imaging]. Zhonghua Yi Xue Za Zhi. 2013;93:816–8. 2013/07/19 ed.
42. Fatu C, Puisoru M, Rotaru M, Truta AM. Morphometric evaluation of the frontal sinus in relation to age. Ann Anat. 2006;188:275–80.
43. Çakur B, Sumbullu MA, Durna NB. Aplasia and agenesis of the frontal sinus in Turkish individuals: a retrospective study using dental volumetric tomography. Int J Med Sci. 2011;8:278–82.
44. Pondé JM, Metzger P, Amaral G, Machado M, Prandini M. Anatomic variations of the frontal sinus. Minim Invasive Neurosurg. 2003;46:29–32.
45. Shah RK, Dhingra JK, Carter BL, Rebeiz EE. Paranasal sinus development: a radiographic study. Laryngoscope. 2003;113:205–9.
46. Matalova E, Fleischmannova J, Sharpe PT, Tucker AS. Tooth agenesis: from molecular genetics to molecular dentistry. J Dent Res. 2008;87:617–23.
47. Barnes E. Developmental Defects of the Axial Skeleton in Paleopathology. University. Colorado; 1994.
48. Schmorl G, Junghans H. In: Besemann E, editor. The Human Spine in Health and Disease. 2nd ed. New York: Grune & Stratton; 1959.
49. Mann R, Verano J. Case report no. 13. Paleopath Newsl 1990;72.
50. Merbs C, Wilson W. Anomalies and pathologies of the Sadlermiut Eskimo vertebral column. Ott Natl Mus Can Bull. 1962;180:154–80.
51. Kamath BM, Loomes KM, Piccoli DA. Medical management of Alagille syndrome. J Pediatr Gastroenterol Nutr. 2010;50:580–6.
52. Anderson PJ, Hall CM, Evans RD, Jones BM, Harkness W, Hayward RD. Cervical spine in Pfeiffer's syndrome. J Craniofac Surg. 1996;7:275–9.
53. Sonel B, Yalçin P, Öztürk EA, Bökesoy I. Butterfly vertebra: a case report. Clin Imaging. 2001;25:206–8.
54. Suzutani T, Ishibashi H, Takatori T. Medico-legal studies on the deaths from coal-mine accidents. 3. Causes of death (author's transl). Hokkaido Igaky Zasshi. 1979;54:479–86.
55. Nerlich AG, Parsche F, Wiest I, Schramel P, Löhrs U. Extensive pulmonary haemorrhage in an Egyptian mummy. Virchows Arch. 1995;427:423–9.
56. Nerlich AG, Bachmeier B, Zink A, Thalhammer SE-VE. Ötzi had a wound on his right hand. Lancet. 2003;362:334.
57. Capanna R, Betelli G, Ruggieri P, Biagini R, Giunti A. Bone cysts of the pelvis. Chir Organi Mov. 1985;70:163–8.
58. Papageorgopoulou C, Suter SK, Rühli FJ, Siegmund F. Harris lines revisited: prevalence, comorbidities, and possible etiologies. Am J Hum Biol. 2011;23:381–91.
59. Viano D, King A. "Biomechanics of Chest and Abdomen Impact.". In: Bronzino JD, editor. Biomed. Eng. Handb. 2nd ed. Boca Raton: CRC Press LLC; 2000.
60. Rühli FJ, Chhem RK, Böni T. Diagnostic paleoradiology of mummified tissue: interpretation and pitfalls. Can Assoc Radiol J. 2004;55:218–27. 2004/09/15 ed.
61. Panzer S, Gill-Frerking H, Rosendahl W, Zink AR, Piombino-Mascali D. Multidetector CT investigation of the mummy of Rosalia Lombardo (1918–1920). Ann Anat. 2013;195:401–8.
62. Villa C, Lynnerup N. Hounsfield Units ranges in CT-scans of bog bodies and mummies. Anthropol Anzeiger. 2012;69:127–45. 2012/05/23 ed.